Human Molecular Genetics, 2008, Vol. 17, No. 2 ***281–292***
doi:10.1093/hmg/ddm304
Advance Access published on October 12, 2007

R91W mutation in Rpe65 leads to milder early-onset retinal dystrophy due to the generation of low levels of 11-*cis*-retinal

Marijana Samardzija[1,*], Johannes von Lintig[2], Naoyuki Tanimoto[3], Vitus Oberhauser[2], Markus Thiersch[1], Charlotte E. Remé[1], Mathias Seeliger[3], Christian Grimm[1] and Andreas Wenzel[1,†]

[1]Laboratory for Retinal Cell Biology, Department of Ophthalmology, University of Zurich, Frauenklinikstr. 24, 8091 Zurich, Switzerland, [2]Institute of Biology I, Animal Physiology and Neurobiology, University of Freiburg, Hauptstr. 1, D-79104 Freiburg, Germany and [3]Ocular Neurodegeneration Research Group, Institute for Ophthalmic Research, University of Tuebingen, Schleichstr. 4/3, D-72076 Tuebingen, Germany

Received September 18, 2007; Revised and Accepted October 10, 2007

RPE65 is a retinal pigment epithelial protein essential for the regeneration of 11-*cis*-retinal, the chromophore of cone and rod visual pigments. Mutations in *RPE65* lead to a spectrum of retinal dystrophies ranging from Leber's congenital amaurosis to autosomal recessive retinitis pigmentosa. One of the most frequent missense mutations is an amino acid substitution at position 91 (R91W). Affected patients have useful cone vision in the first decade of life, but progressively lose sight during adolescence. We generated R91W knock-in mice to understand the mechanism of retinal degeneration caused by this aberrant *Rpe65* variant. We found that in contrast to *Rpe65* null mice, low but substantial levels of both RPE65 and 11-*cis*-retinal were present. Whereas rod function was impaired already in young animals, cone function was less affected. Rhodopsin metabolism and photoreceptor morphology were disturbed, leading to a progressive loss of photoreceptor cells and retinal function. Thus, the consequences of the R91W mutation are clearly distinguishable from an *Rpe65* null mutation as evidenced by the production of 11-*cis*-retinal and rhodopsin as well as by less severe morphological and functional disturbances at early age. Taken together, the pathology in R91W knock-in mice mimics many aspects of the corresponding human blinding disease. Therefore, this mouse mutant provides a valuable animal model to test therapeutic concepts for patients affected by *RPE65* missense mutations.

INTRODUCTION

The vitamin A derivative 11-*cis*-retinal is the chromophore of rod and cone visual pigments. Absorption of light leads to an 11-*cis* to all-*trans* isomerization followed by dissociation of all-*trans*-retinal from the protein moiety (opsin) of the visual pigment holo-complex. The regeneration of the visual chromophore is a complex protein-mediated process termed the visual cycle (1). The crucial all-*trans* to 11-*cis*-retinoid isomerization reaction step takes place in the retinal pigment epithelium (RPE) and is catalyzed by RPE65 (2–4). Rpe65-deficient mice lack 11-*cis*-retinal and consequently no rhodopsin is detectable in their eyes (5,6). Instead, these animals show in the RPE an over-accumulation of retinyl esters, retinoid intermediates of the visual cycle (5).

More than 60 disease-associated mutations have been identified in the human *RPE65* gene [summarized in http://www.retina-international.com/sci-news/rpe65mut.htm; see also Zernant *et al*. (7)]. The broad spectrum of mutations includes point mutations, splice-site defects, deletions and insertions. Mutations in *RPE65* are estimated to account for ~11% of all autosomal recessive childhood-onset retinal dystrophy cases (8). Patients suffering from mutations in the *RPE65* gene are alternatively diagnosed as autosomal recessive retinitis pigmentosa, autosomal recessive retinal dystrophy, early-onset severe retinal dystrophy (EOSRD) or Leber's

*To whom correspondence should be addressed at Tel: +41 442553872; Fax: +41 442554385; E-mail: samam@opht.uzh.ch
†Present address: Novartis Pharma Schweiz AG—BU Ophthalmics, Monbijoustrasse 118, CH-3007 Bern, Switzerland.

congenital amaurosis type II (LCAII) (8–10). These rather diverse diagnoses reflect the phenotypic heterogeneity of the underlying disease. Most patients suffering from mutations in the *RPE65* gene are diagnosed early in childhood as severely visually impaired, with night blindness, distinctly restricted visual fields and nystagmus, but no photophobia (summarized in 11). Retinal function (ERG) is undetectable after dark adaptation and is severely impaired following light adaptation. However, many of these patients have sufficient vision to attend elementary school. Vision is then gradually lost, resulting in blindness almost invariably in the third decade of life (11).

Two naturally occurring models (rd12 mouse and Briard dog) and the genetically engineered Rpe65 knock-out mouse ($Rpe65^{-/-}$) have been useful for the delineation of RPE65 protein function in the visual cycle (5,12,13). These models have meanwhile been used in pre-clinical gene replacement therapy experiments to restore rod and cone photoreceptor function [rd12 (14), $Rpe65^{-/-}$ (15–18), dog (19–22)]. All of the above models represent a 'null situation' for RPE65, in which the visual cycle has never been functional. However, current literature indicates that more than 50% of *RPE65* mutations in patients are missense mutations. Some of these missense mutations presumably produce mutant versions of RPE65 with some residual enzymatic activity. Recently, we characterized three consanguineous families carrying the R91W mutation in *RPE65* (23). All affected family members had useful cone-mediated vision in the first decade of life, suggesting that the mutant RPE65 protein is expressed and possesses residual function. The consequences of a partial loss of RPE65 activity caused by a missense mutation have not yet been studied in an *in vivo* animal model and little is known about the pathology of LCA/EOSRD under such conditions.

To assess this specific pathology, we generated the Rpe65-R91W knock-in mouse as a model for the human disease and analyzed the effect of the mutation on retinal function, visual cycle and morphology.

RESULTS

Generation of R91W knock-in mice

Gene targeting in mouse ES cells was used to modify exon 4 of the Rpe65 gene such that codon 91 changed from arginine to tryptophan (R91W) (Fig. 1A). In humans, the R91W mutation is caused by a single point mutation (TGA>TGG). However, in mice, arginine 91 is encoded by a CGA codon; therefore, two point mutations were introduced into codon 91 (CGA>TGG). The introduction of these two mutations resulted in the loss of a *Taq*I restriction site, facilitating the genotype analysis (Fig. 1A–C).

The gene targeting strategy is shown in Figure 1B. In addition to mouse Rpe65 genomic DNA carrying the R91W mutation, the targeting vector contained a floxed neo resistance and a diphtheria toxin (DT) cassette as selection markers. Sequencing of the full genomic DNA insert of the targeting vector confirmed the presence of the R91W mutation and the selection markers in an otherwise wild-type sequence (Fig. 1A). The linearized construct was electroporated into coisogenic TC1 ES cells, and correctly targeted ES cell clones were identified and characterized in detail by Southern blotting, PCR and PCR restriction digestion analysis (Fig. 1C; data not shown).

These clones were used to generate germ-line competent chimeric mice. A chimeric male was mated with coisogenic 129S6 females to propagate the line. The resulting heterozygous ($Rpe65^{R91Wneo}$) F1 mice were bred with a germ-line Cre-deleter mouse line [129S6-Tg(Prnp-GFP/Cre)1Blw/J)] (24) to excise the neo cassette (Fig. 1B). The resulting offspring was heterozygous for the R91W mutation (R91W/wt). The only foreign sequence in addition to the R91W substitution was a single intronic *lox*P site. Finally, we interbred the heterozygous R91W/wt mice to obtain pure homozygous 129S6/SvEvTac-$Rpe65^{tm1Lrcb}$ (R91W) knock-in mice. Of note, these mice were coisogenic to 129S6 control mice, except for codon 91 and the above-mentioned *lox*P site.

Rpe65 expression in mutant mice

Quantitative RT–PCR, immunoblotting and immunohistochemistry showed that the mutant protein is expressed in R91W knock-in but not in $Rpe65^{-/-}$ mice (Fig. 2A–C). Whereas the expression of Rpe65 mRNA was only slightly reduced in R91W mice (Fig. 2A), immunoblotting revealed that the steady-state protein levels of the $RPE65^{R91W}$ mutant variant were reduced by 95% when compared with wild-type mice (Fig. 2B; data not shown). The mutant protein was detected in the RPE and thus was correctly localized (Fig. 2C).

Lecithin retinol acyltransferase (LRAT) and cellular retinaldehyde binding protein (CRALBP) are functionally connected to RPE65 and the visual cycle (25–28). Expression of both proteins was comparable in eyecups of 8-week-old wild-type, R91W knock-in and $Rpe65^{-/-}$ animals with a tendency of increased LRAT levels in knock-out mice (Fig. 2B). Levels of rod opsin were slightly reduced in retinas of R91W mice and—as previously reported (5)—in retinas of $Rpe65^{-/-}$ animals.

Retinoid analysis

The absence of RPE65 results in the arrest of the visual cycle, causing an accumulation of retinyl esters in the RPE and visual chromophore deficiency (5). On the basis of this observation, we expected that the dramatically reduced protein levels of the $RPE65^{R91W}$ variant (Fig. 2B) would also result in a disturbance of the visual cycle. Therefore, we analyzed the retinoid composition in dark-adapted wild-type, R91W/wt heterozygous, R91W homozygous and $Rpe65^{-/-}$ mice at different ages. HPLC analysis of whole eye preparations of 4, 8, 12, 24 and 40-week-old animals demonstrated the presence of 11-*cis*-retinal in R91W homozygous mice, though at low levels between 2.5 and 6.3% when compared with age-matched wild-type animals (Table 1). As expected, no 11-*cis*-retinal was detectable in $Rpe65^{-/-}$ mice at any age (Table 1) (5,29). All-*trans*-retinal, all-*trans*-retinol and 9-*cis*-retinal levels were comparable between R91W and $Rpe65^{-/-}$ mice. The retinoid content and composition in R91W/wt heterozygous animals did not differ from wild-type mice at all tested ages (Table 1).

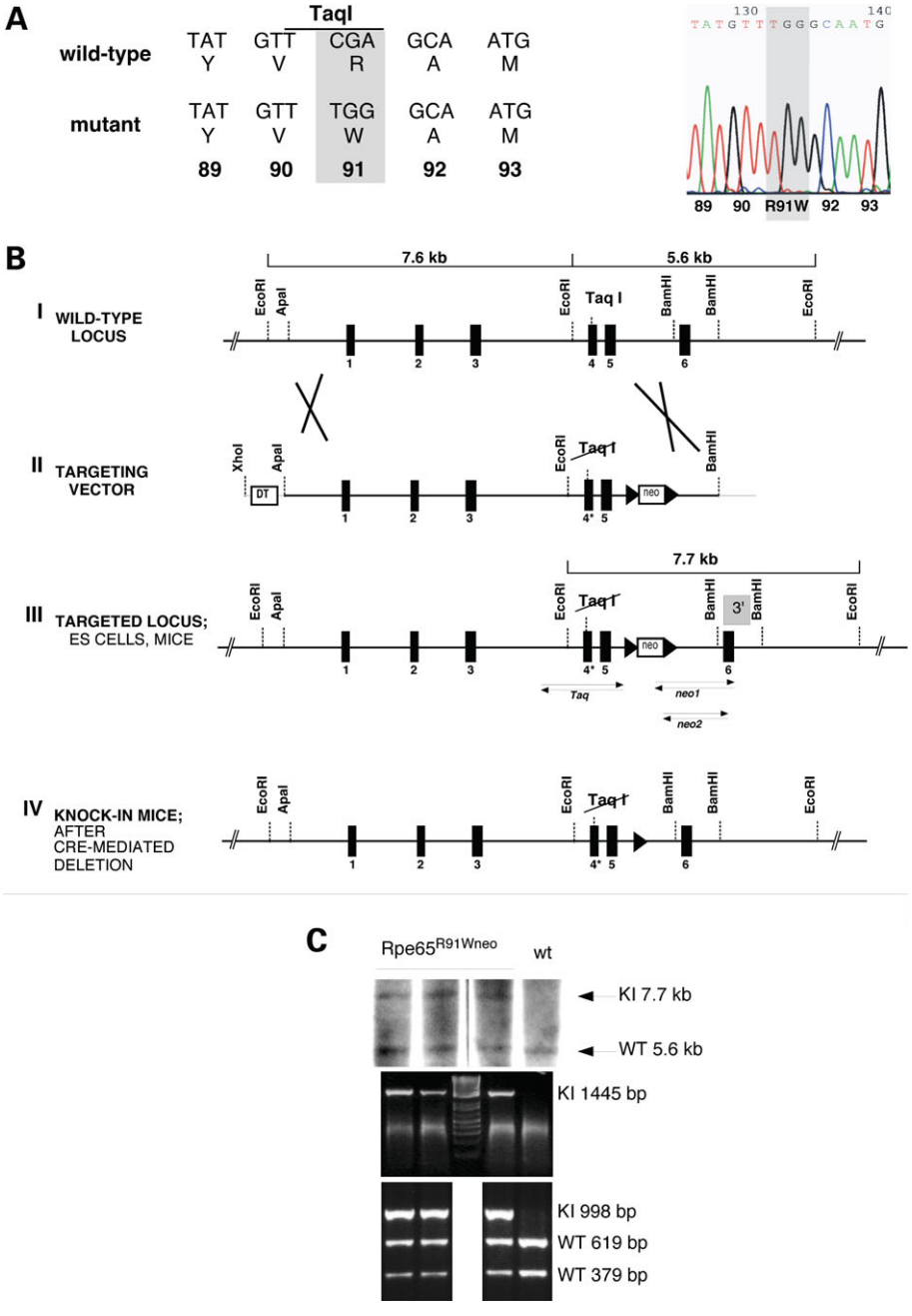

Figure 1. Generation of R91W knock-in mice. (**A**) Partial sequence of exon 4 wild-type and mutated R91W DNA. Note that two point mutations were introduced in the codon for arginine (R) at position 91 to obtain tryptophan (W). This resulted in the loss of a *Taq*I restriction site in the mutated DNA (right panel). Sequence data of the targeting vector showing the mutant TGG triplet at position 91 (left panel). (**B**) Schematic representation of the R91W targeting strategy I: partial wild-type *Rpe65* allele, with restriction enzyme sites and location of first six exons (boxes). II: targeting construct containing R91W mutation (indicated as lost *Taq*I restriction site in mutated exon 4*), neomycin (neo)-resistant gene flanked by *lox*P sites (indicated as triangles) suitable for cre-medated excision, and diphtheria resistance cassette (DT). Note the unique *Xho*I restriction site used for linearization of the targeting vector. III: genomic *Rpe65* DNA after integration of targeting vector carrying the neomycin cassette ($Rpe65^{R91Wneo}$). Positions of PCR primer pairs and Southern blot probe (gray box) for PCR are indicated. Neo1 and neo2 are nested primer pairs designed to read from the selection cassette into the 3′ short arm outside of targeting area. These primers were used to confirm the HR. The *Taq* primer pair was used to confirm the presence of R91W mutation (see Materials and Methods). IV: the partial R91W mutant allele after the removal of the neo cassette by crossing $Rpe65^{R91Wneo}$ mice with the Cre-deleter mice. (**C**) Genotyping of R91W mutants. Upper panel: DNA was isolated from neomycin-resistant ES cell colonies and analyzed by Southern blotting, after digestion with *Eco*RI, and using 3′external probe as indicated in (B). Signal from the genomic DNA from wild-type (wt) allele is 5.6 kb. A heterozygous $Rpe65^{R91Wneo}$ knock-in (KI) allele gives rise to additional 7.7 kb due to the presence of the neomycin cassette. Middle panel: PCR analysis of the same DNA using neo1 and neo2 nested primer pair. A PCR fragment of 1445 bp detected in heterozygous $Rpe65^{R91Wneo}$ knock-in due to the presence of the neomycin cassette. Lower panel: RFLP-PCR analysis of the same DNA using the *Taq* primer pair [see (B)]. A PCR fragment of 998 bp was digested with the *Taq*I restriction enzyme. In wild-type animals, this results in a 379 and a 619 bp fragment. Heterozygous $Rpe65^{R91Wneo}$ knock-in DNA contains an additional 998 bp fragment due to the loss of the *Taq*I restriction site. This protocol was used for genotyping of the final R91W knock-in mice. Asterisk indicates mutated exon 4.

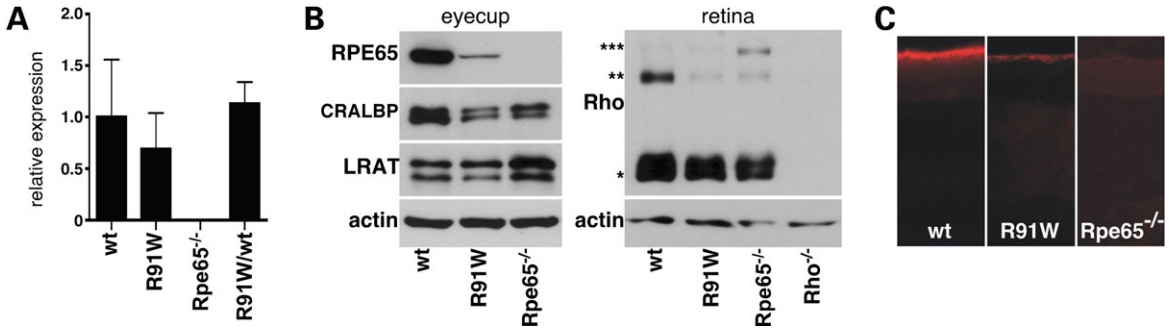

Figure 2. R91W mutation causes reduced levels of RPE65. (**A**) Relative mRNA levels of Rpe65 expressed in eyecups of wild-type, R91W (homozygous), $Rpe65^{-/-}$ and R91W/wt (heterozygous) mice at 8 weeks of age as determined by real-time RT–PCR. mRNA levels, normalized to β-actin, are expressed relative to wild-type control, which was set to 1. RNA isolated from three independent retinas per age and genotype was amplified in triplicates (means ± SD). (**B**) Western blotting of eyecup or retinal proteins from 8-week-old wild-type, R91W or $Rpe65^{-/-}$ mice. The presence of the R91W mutation resulted in reduced amounts of RPE65 immunoreactivity. Note similar levels of LRAT and CRALBP in the eyecups of all strains with a tendency of increased LRAT levels in $Rpe65^{-/-}$ mice. Slightly reduced amounts of rod opsin (Rho) were detected in retinas of mutant mice (asterisk indicates Rho monomer, dimer or trimer, respectively). Shown are the representative blots from at least three different animals per genotype. (**C**) Immunolabeling with a polyclonal antibody to RPE65, demonstrating that the $RPE65^{R91W}$ mutant protein is expressed only in RPE cells. Note the reduced immunoreactivity when compared with animals expressing wild-type RPE65 protein. The $Rpe65^{-/-}$ animals served as negative controls.

Table 1. Retinoid analysis

	Age	11-*cis*-retinal	All-*trans*-retinal	All-*trans*-retinol	Retinyl ester	9-*cis*-retinal
Wild-type	4	380.2 ± 60.1	39.0 ± 11.3	4.2 ± 3.6	30.6 ± 5.6	n.d.
	8	336.1 ± 21.8	34.7 ± 1.6	5.4 ± 9.4	39.2 ± 5.0	n.d.
	12	336.7 ± 32.4	62.6 ± 12.9	n.d.	34.9 ± 4.6	n.d.
	24	373.6 ± 75.5	47.9 ± 3.7	2.2 ± 3.8	106.2 ± 27.2	n.d.
R91W/wt	4	394.7 ± 22.6	53.4 ± 7.1	6.0 ± 0.8	44.3 ± 5.4	n.d.
	8	371.8 ± 22.1	87.1 ± 4.7	n.d.	55.7 ± 8.4	3.7 ± 0.3
	12	454.8 ± 42.0	52.4 ± 5.5	3.0 ± 3.7	89.6 ± 17.9	n.d.
	24	337.4 ± 49.0	86.4 ± 15.3	n.d.	108.9 ± 23.3	n.d.
R91W	4	24.0 ± 3.0	3.6 ± 0.6	10.4 ± 1.9	420.7 ± 34.5	7.6 ± 0.8
	8	15.4 ± 0.2	4.8 ± 1.5	9.2 ± 5.2	651.9 ± 127.4	9.9 ± 0.9
	12	13.5 ± 0.2	2.7 ± 0.4	13.9 ± 2.7	1542.7 ± 271.8	9.2 ± 1.2
	24	9.4 ± 8.2	1.9 ± 1.7	20.2 ± 17.7	2186.1 ± 160.1	4.3 ± 3.7
	40	18.2 ± 4.8	2.2 ± 1.0	12.4 ± 3.4	2107.9 ± 138.9	10.6 ± 3.2
$Rpe65^{-/-}$	4	n.d.	n.d.	8.6 ± 2.5	271.4 ± 22.8	4.8 ± 1.5
	8	n.d.	1.3 ± 1.2	5.4 ± 1.0	474.9 ± 49.1	8.5 ± 0.7
	12	n.d.	1.9 ± 0.4	14.9 ± 4.1	805.9 ± 57.5	6.7 ± 0.9
	24	n.d.	2.1 ± 0.3	8.5 ± 4.8	1160.6 ± 529.0	10.3 ± 3.8
	40	n.d.	2.8 ± 1.0	15.6 ± 5.1	2622.9 ± 531.3	13.1 ± 11.2

All values are given in pmol/eye ± SD ($n = 3$). Age in weeks, as indicated. n.d., not detectable.

The presence of 11-*cis*-retinal indicated that the visual cycle is functional in R91W animals. Nevertheless, we detected a strong and almost linear (13 pmol/day; $R^2 = 0.93$) accumulation of retinyl esters during the first 24 weeks of life. Between 24 and 40 weeks, no further increase was detected (2186 and 2108 pmol/eye, respectively; Table 1) suggesting that a plateau was reached in R91W mice. In $Rpe65^{-/-}$ animals retinyl ester levels increased linearly (9 pmol/day; $R^2 = 0.96$) throughout 40 weeks (Table 1). Electron microscopy revealed that this accumulation of retinyl esters was accompanied by the formation of lipid droplets in the RPE of R91W and, as previously reported, in $Rpe65^{-/-}$ mice (5) (Fig. 3).

Rhodopsin content and regeneration

We next determined dark-adapted rhodopsin levels, which reached 30 pmol/retina (Fig. 4A) in R91W mice representing 6% of wild-type rhodopsin. This percentage was comparable to the amount of 11-*cis*-retinal observed in 4-week-old R91W mice, which corresponded likewise to 6% of wild-type levels (Table 1).

The expression levels of RPE65 protein govern the kinetics of rhodopsin regeneration (30,31). Given the reduced amount of RPE65 in R91W mice (Fig. 2), we expected that rhodopsin would regenerate with a much slower rate. To allow a maximal rhodopsin production, we kept R91W mice in darkness for 4, 10 and 22 days. By the time of analysis, the mice were 6–7-weeks old. Maximal rhodopsin levels detected after 22 days in darkness were 42 pmol, which was still <10% of wild-type animals (Fig. 4A; see Fig. 4C for the wild-type levels).

In order to test rhodopsin regeneration kinetics, 6–7-week-old animals were dark-adapted for 24 h and exposed for 10 min to 5000 lux, which bleaches 90% of rhodopsin in

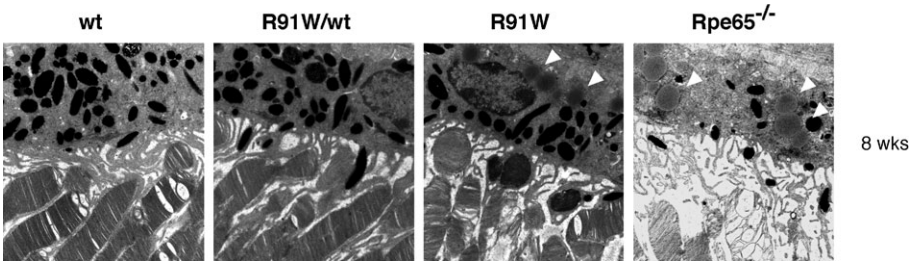

Figure 3. Lipid-like inclusions in R91W mice. Electron microscopy of the RPE-photoreceptor interface in 8-week-old wt, R91W/wt, R91W and Rpe65$^{-/-}$ mice. Note that lipid-like inclusions (arrowheads) are present in R91W and Rpe65$^{-/-}$ mice only, and the better preservation of OS morphology in R91W mice when compared with Rpe65$^{-/-}$.

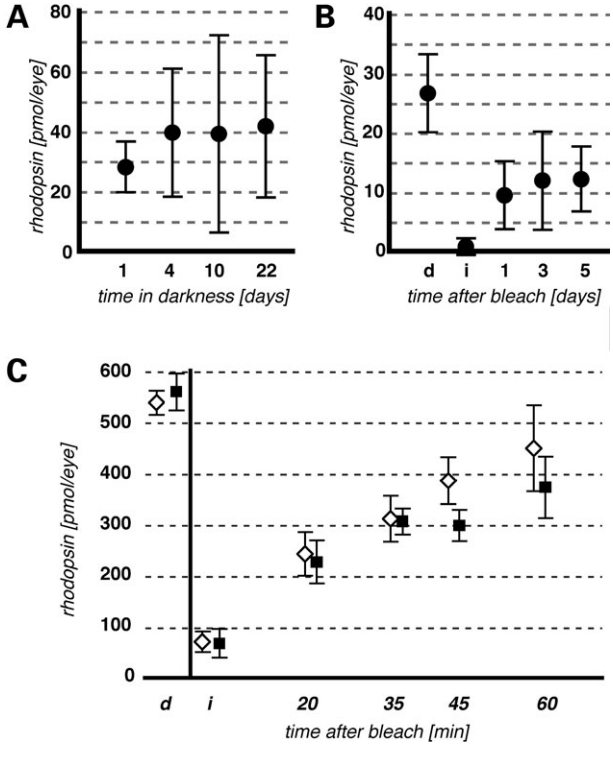

Figure 4. Rhodopsin content and regeneration kinetics. (**A**) Rhodopsin levels in 6–7-week-old R91W animals kept in darkness for 1 day or up to 22 days (as indicated). (**B**) Rhodopsin regeneration of R91W and wild-type mice. Following 24 h dark-adaptation, R91W mice were exposed to 5000 lux for 10 min and the rhodopsin content was analyzed either immediately (i) or after different periods of recovery in darkness (as indicated). Unexposed, dark-adapted mice (d) served as controls. (**C**) Rhodopsin regeneration of wild-type and R91W/wt heterozygous mice. Experimental protocol and abbreviations are as in (B). Note the slightly slower regeneration kinetics in R91W/wt mice. Filled squares, R91W/wt; open squares, wild-type. All values are given in pmol/eye ± SD. At least three animals per condition and genotype were analyzed.

wild-type mice (27). Animals were returned to darkness to allow regeneration of the visual pigment. Non-exposed R91W mice contained 27 pmol of rhodopsin (Fig. 4B), which was bleached by light exposure, reducing it to 1 pmol. Even after prolonged dark-adaptation (5 days) only 44% (12 pmol) of the pre-bleach value (27 pmol) was detectable. Thus, following a strong bleach, regeneration of rhodopsin was inefficient and reached a plateau at about half the maximal level of non-bleached, dark-adapted animals. Maximal dark-adapted rhodopsin levels were similar in R91W/wt heterozygous (538 pmol/retina) and wild-type (560 pmol/retina) (Fig. 4C). The calculated regeneration rates following a strong bleach were 6.3 pmol/min in wild-type and 4.9 pmol/min in R91W/wt mice, indicating slightly slower rhodopsin regeneration kinetics in the heterozygous situation.

Photoreceptor function in R91W mutant mice

Next, we studied the consequences of the reduced 11-*cis*-retinal levels on retinal function. Scotopic ERG recordings revealed that higher flash intensities were needed to induce an electrical response in R91W when compared with wild-type mice (Fig. 5A, top panel). By assessing the luminance required to generate a half maximal b-wave amplitude (32), the reduction in light sensitivity in 8-week-old R91W mice was determined to be ~2.5 log units when compared with wild-type. Therefore, R91W mice are about one log unit more sensitive to light than Rpe65$^{-/-}$ animals (6). In age series testing of 8, 12, 24 and 40-week-old animals, the sensitivity threshold remained unaltered, whereas the b-wave amplitude was reduced with increasing age in R91W, this being especially prominent between 12 and 24 weeks (Fig. 5A, top and bottom panels). From 24 to 40 weeks of age, no further reduction in b-wave amplitude was detected. Thus, the sensitivity of the retina was not prone to age-related reduction, whereas the maximal response size was.

In order to test cone function, ERG responses were recorded under photopic conditions (Fig. 5B). Notably, there was no difference in threshold sensitivity or in amplitude of the b-wave between 8-week-old R91W and wild-type control animals (Fig. 5B, top and bottom panels). Given the low amount of chromophore available (Table 1), cone responses should be somehow affected. In addition, the waveforms were altered in a way similar to that observed in *Rpe65* null mice (6), indicating that rods are active under those conditions. Therefore, it appears that the photopic signals are mixed responses containing both rod and cone system components.

A comparison of wild-type and R91W/wt heterozygous animals resulted, as expected, in no difference between the genotypes under scotopic or photopic conditions (data not shown).

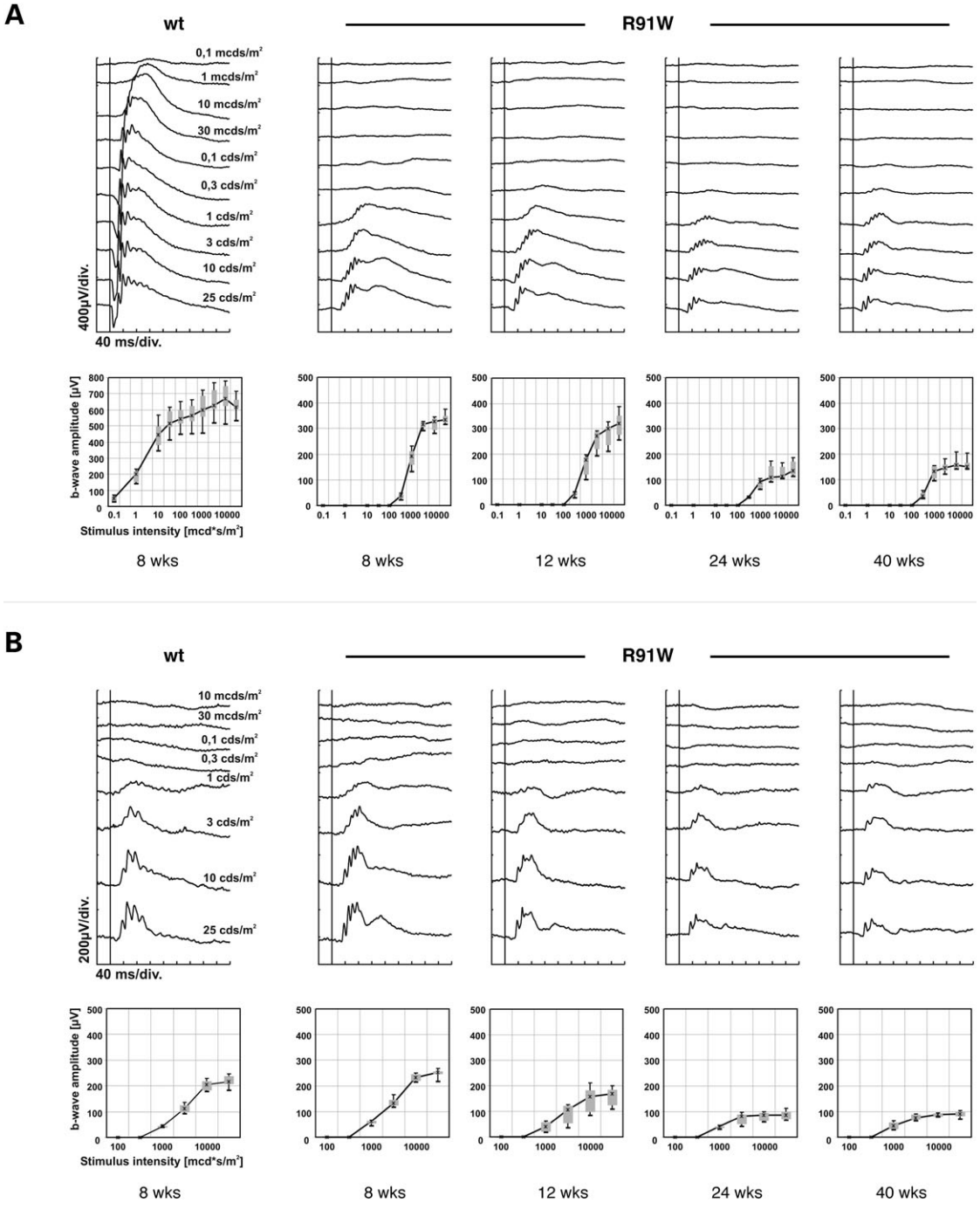

Figure 5. ERG responses to single-flash stimuli with increasing intensities in 8, 12, 24 and 40-week-old R91W and wild-type animals. (**A**) Scotopic single-flash ERG intensity series indicating loss of sensitivity in mutant mice. (**B**) Photopic single-flash ERG intensity series reflecting a similar sensitivity of wild-type and R91W animals at 8 weeks of age. Note the decline of the b-wave amplitude with increasing age. Upper panels in (A) and (B) are recordings from representative animals for a given genotype and age and in lower panels group statistics are presented ($n = 3$). Boxes in group statistic graphs indicate the 25 and 75% quantile range, whiskers indicate the 5 and 95% quantile, and the black line connects the medians of the data.

Assessment of retinal morphology

The results of the tests for retinal function, both scotopic and photopic ERG responses, in R91W mice suggested an age-related retinal degenerative process (Fig. 5). To analyze the consequences of the R91W mutation on retinal morphology, we compared the three different genotypes (wild-type, R91W and Rpe65$^{-/-}$) at various ages (from 4 weeks to 1 year; Fig. 6). Already at 4 weeks of age, the outer segments (OS) of R91W and Rpe65$^{-/-}$ mice showed signs of disorganization (Fig. 6, top row). The reduced compactness and shortening of OS became more obvious as mice grew older. Although the thickness of the outer nuclear layer (ONL) at earlier time-points was comparable with wild-type,

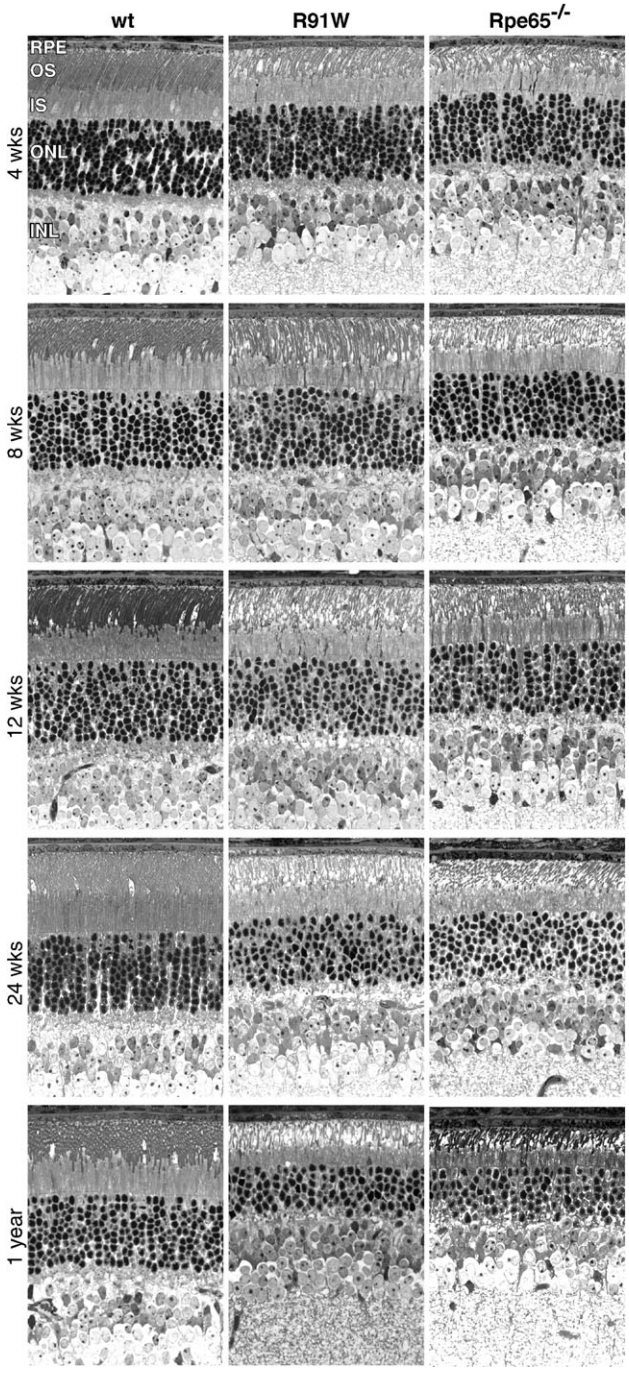

Figure 6. Light microscopic changes in R91W retinas in comparison to wild-type and Rpe65$^{-/-}$ mice at various ages. Disorganization of OS was evident in R91W mice already at 4 weeks and became more pronounced with aging. By 8 weeks, more voids were visible in the ONL accompanied by the appearance of pycnotic nuclei. By 1 year, only five to six rows of nuclei remained in the ONL. When compared with Rpe65$^{-/-}$ mice, R91W mice showed better retinal preservation (longer OS and higher density) and more cone nuclei were visible in younger animals. RPE, retinal pigment epithelium; OS, outer segments; IS, inner segments; ONL, outer nuclear layer; INL, inner nuclear layer.

only five rows of nuclei remained in the central area of 1-year-old mutant animals, when compared with nine to 10 rows in 1-year-old wild-types. In comparison to Rpe65$^{-/-}$ animals, R91W mice showed a better preservation of OS, at least up to 12 weeks of age (Fig. 6). Notably, R91W mice contained more cone nuclei than respective age-matched Rpe65$^{-/-}$ mice, particularly at early age.

At all ages, we found no differences between the retinal morphology of wild-type and R91W/wt heterozygous mice (data not shown), which is in line with a recessive inheritance of the phenotype caused by the R91W mutation. Furthermore, no morphological differences between genotypes were detectable in inner retinal structures upon examination by light microscopy.

DISCUSSION

R91W knock-in mice phenocopy human disease

In humans, about half of the identified mutations in *RPE65* are missense mutations [http://www.retina-international.com/sci-news/rpe65mut.htm; see also Zernant *et al*. (7)]. The newly generated Rpe65 R91W knock-in mice represent the analogous animal model to human patients carrying a missense mutation in *RPE65*. In patients, the different mutations in *RPE65* are associated with variable degrees of severity of retinal dysfunction (10,33). This is likely explained by the different functional consequences of these mutations. All presently available animal models, however, carry either null mutations having no residual function or a variant (L450M) which causes only a mild disturbance of the visual cycle without retinal degeneration (34).

We found that the rod system in R91W knock-in mice is severely desensitized, although not as much as in mice lacking RPE65 (6). Cones, however, are better preserved and appear to be functional at least in young animals. Similarly, R91W patients diagnosed with EOSRD are typically night-blind (desensitized rod system) but retain cone-mediated vision in the first decade (23). Reports on patients carrying other missense mutations in *RPE65* demonstrate functional cone vision early in life (summarized in 35). Another distinct group of patients affected by *RPE65* mutations is characterized as legally blind from birth or severely visually impaired in infancy. These patients are diagnosed as LCAII. The corresponding mouse model, Rpe65$^{-/-}$ mice, clearly has no cone function, and the minimal residual visual function is due to desensitized rods using isorhodopsin with 9-*cis*-retinal as a chromophore (6,36). The R91W knock-in mice, like patients suffering from EORSD, possess a phenotype clearly distinguishable from the null situation in both mice and humans. Thus, our analysis suggests that for an understanding of a particular disease, reproducing the real mutation is superior to a 'simple' knock-out mouse model.

Metabolic changes induced by R91W mutation

Very recently, the role of RPE65 as the isomerohydrolase in the visual cycle was demonstrated by studies in cell culture systems (2–4,37). In these experiments, a minimal visual cycle has been restored in cell lines different from RPE and only cells transfected with RPE65 vectors produced 11-*cis*-retinal from precursor molecules. Further studies using the same experimental paradigm aimed at the understanding of

the consequences caused by missense mutations in *RPE65* related to human disease (4,38,39). In particular, a study on *RPE65*^{R91W} showed that this mutation causes decreased protein levels due to a decreased protein stability and/or protein mislocalization (39). Additionally, in this report no isomerohydrolase activity of the RPE65^{R91W} protein variant was detected. To circumvent the limitations of the *in vitro* cell culture system and to analyze the consequences of RPE65 missense mutations in a more 'natural' environment, Chen *et al*. (17) employed a different strategy: they delivered mutant Rpe65 genes to the RPE of RPE65-deficient mice by means of an adenoviral vector. This strategy reproduced the results of the *in vitro* cell culture system. In particular, the expression of Rpe65^{R91W} did not result in detectable RPE65 immunostaining in the RPE and accordingly was not accompanied by 11-*cis*-retinal production or a gain of retinal function.

In contrast, R91W knock-in mice showed: (i) detectable protein expression with a correct localization to the RPE and (ii) metabolic activity as evidenced by the generation of 11-*cis*-retinal. Thus, not surprisingly, the *in vivo* situation represents the most accurate model to assess the consequences of a mutation. This study also validates our hypothesis that the RPE65 protein with an R91W amino acid substitution possesses residual activity in human patients.

R91W knock-in mice have an altered visual cycle

Like the wild-type protein, the mutant RPE65^{R91W} was detected exclusively in the RPE, but at highly reduced levels (5% of wild-type levels). Since RNA levels were less affected (-40%), translational or post-translational mechanisms may contribute to the reduction in the protein levels of the RPE65^{R91W} variant. Comparison of Rpe65 knock-out with Rpe65 R91W knock-in mice revealed important differences with regard to biochemical function, the most important one being the limited, but measurable ability of R91W knock-in mice to generate 11-*cis*-retinal. In order to form functional rhodopsin, 11-*cis*-retinal has to be incorporated into rod opsin. In wild-type mice, the levels of 11-*cis*-retinal and rod opsin are linearly correlated (27). In R91W mice, rod opsin was only slightly reduced in comparison to wild-type animals (Fig. 2B). Thus, low amounts of rod opsin are not the reason for reduced 11-*cis*-retinal and rhodopsin levels ($<10\%$ of wild-type). Another limitation of the visual cycle in R91W knock-in mice was revealed in bleaching experiments. Wild-type mice recovered their rhodopsin within 1–3 h after a bleach (27,34). R91W mice did not recover rhodopsin to dark-adapted levels within days. Thus, in addition to the limitation in rhodopsin production as outlined above, a strong bleach impaired rhodopsin regeneration.

Our data suggest that large amounts of unliganded rod opsin must be present in photoreceptors of R91W knock in mice, despite the fact that R91W mice can produce 11-*cis*-retinal. As 11-*cis*-retinal acts as an inverse agonist, its low availability could cause increased spontaneous activity of the chromophore-free opsin molecule, leading to a constitutive activation of the phototransduction cascade (40,41). It has been hypothesized that in the presence of unliganded opsin the retina sends a signal that results in vitamin A uptake from the circulation (26). Thus, an insufficient supply of opsin with 11-*cis*-retinal in R91W mice may be the cause of the observed accumulation of retinyl esters.

One might speculate that 11-*cis*-retinal in R91W mice does not originate from RPE, but from the recently proposed cone visual cycle (42). In this alternate pathway, the cone pigment is regenerated in Müller glia cells, independently of the RPE. Hypothetically, such a cone visual cycle could be less affected, or even may be fully operational despite the R91W mutation. But how would the rods acquire 11-*cis*-retinal under this condition? 11-*cis*-retinal is covalently bound to rod opsin via a protonated Schiff base and this binding is tight. The cone opsin/11-*cis*-retinal holocomplex is less stable, and it has been recently shown to dissociate spontaneously (43). Thus, 11-*cis*-retinal might be 'stolen' by rods from cones due to this spontaneous dissociation of the visual chromophore. This scenario might also explain why rhodopsin regeneration kinetics is inefficient. Even though RPE65 has been reported to be detected in cones (44,45) and this disputed (6,46), there is no experimental evidence that RPE65 is directly involved in the proposed cone visual cycle. However, contradictory to this hypothesis, almost equal amounts of 11-*cis*-retinal were retained up to 40 weeks of age, the time when the cones in R91W animals are almost completely lost (unpublished data).

Retinal degeneration

Constant activation of the phototransduction cascade due to chromophore starvation has been implicated in rod degeneration in Rpe65$^{-/-}$ mice and consequently rod degeneration can be prevented by blocking rod specific G-protein transducin (Gnat1) signaling (47). Nevertheless, Rpe65$^{-/-}$; Gnat1$^{-/-}$ double mutant animals accumulate similar amounts of retinyl esters as Rpe65$^{-/-}$ mice, indicating that unliganded opsin, and not the accumulation of retinyl esters, is the primary cause of degeneration (47). This concept is reinforced by the observation that systemic supplementation with 9-*cis*-retinal preserves photoreceptor structure, despite continuing accumulation of retinyl esters (26). Accordingly, a better preservation and slower degeneration of retinal morphology in R91W in comparison to Rpe65$^{-/-}$ animals might be attributable to the presence of small amounts of 11-*cis*-retinal. Nevertheless, also in R91W mice, the phototransduction cascade may be permanently activated, finally causing retinal degeneration. This possibility will be further investigated in R91W; Gnat1$^{-/-}$ double mutant mice.

Conclusion

We generated a novel mouse model for retinal dystrophy caused by a missense mutation in RPE65. There are striking functional differences to the knock-out situation, which are not only important for basic research but also for understanding the pathology and for clinical diagnosis in patients. Furthermore, our results indicate that the therapeutic window for gene therapy—the first tests of which are being carried out these very days—is likely to differ between patients with

null and missense mutations. Thus, preclinical trials for gene replacement are underway for the R91W knock-in mouse.

MATERIALS AND METHODS

Generation of R91W knock-in mice

A classical strategy using homologous recombination (HR) in embryonic stem (ES) cells has been employed to replace the wild-type with a modified Rpe65 allele; 13.3 kb of Rpe65 genomic DNA (derived from the 129/Sv mouse strain) divided into two contiguous subclones: E1-12 containing exons 1–3 and clone E2-8 containing exons 4–6 cloned into *Eco*RI restriction site of pBluescriptII SK(−) vector were kindly provided by M.T. Redmond (National Eye Institute, Bethesda, USA) (48).

Clone E2-8 containing exon 4 served as template for the PCR targeted site-directed mutagenesis. Two point mutations were introduced into the mouse R91 codon (CGA > TGG) using a respective reverse primer (C AGT CAT TGC CCA AAC ATA AGC ATC AGT GCG GAT GAA TCT GAA GAC TAT TGA GAA ATG GA; underlined codon denotes position 91) to obtain the R91W mutation. The forward primer (GCG CGT AAT ACG ACT CAC TA) was designed to hybridize in the plasmid backbone. The presence of the R91W mutation was confirmed by sequencing. The neomycin (neo) resistance cassette flanked by *lox*P sites (floxed-neo) in the direct repeat orientation was integrated into the *Nhe*I site downstream exon 5. The 3′ site of the vector was truncated by *Bam*HI digestion resulting in the creation of the short arm of the targeting construct. In the final step, the DT cassette was introduced at the 5′ site of the vector (upstream of exon 1) to serve as a negative selection marker. The final targeting construct carrying the R91W mutation was sequenced.

The *Xho*I-linearized targeting vector was electroporated into coisogenic TC1 ES cells derived from 129S6/SvEvTac (129S6) mouse strain (49). Genomic DNA from G418-resistant ES clones was analyzed for correct vector integration by PCR and Southern blotting as described below.

The positive ES clones were injected into blastocysts originating from C57BL/6 mice to obtain chimeric mice. Two chimeric males were born. Germ-line transmission was confirmed in one male. This was done by breeding the chimeric males with C57BL/6 females where positive selection was performed by coat colour assessment and PCR genotyping form tail genomic DNA using neo1, neo2 and *Taq* primer pairs (Table 2).

Following the confirmation of germ-line transmission, the chimeric male was bred to 129S6 females to propagate the line on a coisogenic background. This breeding resulted in the generation of a heterozygous $Rpe65^{R91Wneo}$ line. The genotype was confirmed by PCR using neo1, neo2 and *Taq* primer pairs (Table 2).

For *in vivo* removal of the neo resistance cassette, $Rpe65^{R91Wneo}$ mice were bred with deleter mice expressing cre recombinase in their germ-line [129S6-Tg(Prnp-GFP/Cre)1Blw/J (24)]. The $Rpe65^{R91Wneo}$ mice were kept on a cre-deleter background for two generations to ensure complete excision of the floxed-neo cassette. The deletion of the neo cassette was confirmed by PCR genotyping using neo1, neo2 and cre primer pairs (Table 2). Finally, the resulting heterozygous (R91W/wt) offspring was intercrossed to obtain R91W homozygous mice. The R91W knock-in mice analyzed herein were therefore on a coisogenic 129S6 background. The genotyping of the final R91W knock-in mice was performed by PCR on tail genomic DNA using the *Taq* primer pair as described in Table 2.

Genotype assessment

DNA from G418-resistant ES cells was analyzed by Southern blotting. An external 3′ *Bam*HI probe (759 bp) was random-labeled using the DIG labeling kit (#1585614, Roche Diagnostics, Mannheim, Germany). Genomic ES cell DNA was digested overnight with *Eco*RI and electrophoresed on a 0.8% agarose gel. DNA samples were transferred onto a nylon membrane by a capillary method. The membrane was incubated with the DIG-labeled probe. Fragments corresponding to wild-type and, knock-in alleles (5.6 and 7.7 kb, respectively) were detected by enhanced chemiluminescence.

For the detection of the correctly integrated neo cassette, two primer pairs have been selected to allow a nested PCR approach (Table 2). For the neo1 primer pair, the forward primer was designed within the neo cassette and the reverse primer was positioned outside of the targeted DNA sequence. To further minimize any false-positive result, a nested neo2 primer pair was created within the same area, thus only correctly integrated DNA should be detectable by PCR (Table 2).

A *Taq* primer pair (Table 2) was used to detect the presence of the R91W mutation. This pair produced a 998 bp fragment from both wild-type and mutant DNA. Only the wild-type DNA amplicon included a *Taq*I restriction site, resulting in 619 and 379 bp fragments after incubation with *Taq*I restriction enzyme.

Animals

All procedures concerning animals were in accordance with the regulations of the Veterinary Authority of Zurich and with the statement of 'The Association for Research in Vision and Ophthalmology' for the use of animals in research. All animals were raised in cyclic light (12:12 h; 60 lux at cage level). The cre expressing mice 129S6-Tg(Prnp-GFP/Cre)1Blw/J (24) and corresponding wild-type mice (129S6) were purchased from the Jackson Laboratory (Bar Harbor, USA). Rpe65 deficient mice ($Rpe65^{-/-}$) were maintained at the University Hospital Zurich (5). Genotyping was performed by PCR on tail genomic DNA, using the primers shown in Table 2.

RNA isolation, reverse transcription and real-time PCR

RNA isolation and reverse transcription from eyecup tissue were performed as previously described (50). cDNA quantification was carried out by real-time PCR using the LightCycler 480 Sybr Green I Master kit and a LightCycler 480 instrument (Roche). cDNAs were amplified with primers for Rpe65 and β-actin described elsewhere (5,51), and normalization was done using the ΔΔCT (comparative threshold cycle) method. Relative values were calculated using a suitable calibrator

Table 2. PCR primers used for genotyping

Primer	Forward (5′–3′)	Reverse (5′–3′)	Size (bp)
neo1[a]	AGCAGCCTCTGTTCCACATAC	GATGAGCAGTGGCACCATTG	1513
neo2[a]	CTCAGTATTGTTTTGCCAAG	GATCAACCTGTAGAATGAAAG	1445
Cre	GGACATGTTCAGGGATCGCCAGGCG	GCATAACCAGTGAAACAGCATTGCTG	268
Taq[b]	GCTGGTCTTGCCTGTATCA	GTCAGAGACAGTGCTGTGTT	998

[a]The genotyping using neo1 and neo2 included: a first PCR using the neo1 primer pair amplified for 20 cycles followed by the nested PCR using neo2 primer pair amplified for 35 cycles.
[b]*Taq* primer pair used to genotype R91W mice. Genotyping included digestion of the 998 bp PCR product by *Taq*I restriction. This digestion results in generation of 619 and 379 bp fragments in wild-type animals, or no cleavage in R91W knock-in animals.

sample as indicated in the results. Three animals were analyzed per genotype and each reaction was run in triplicate.

Western blotting

The retina or the remaining eyecup tissue was separately isolated and processed for immunoblotting as previously described (27). The primary antibodies used were: rabbit anti-RPE65 (pin5; 1:2000); mouse anti-LRAT (1:1000, gift from K. Palczewski, University of Washington, Seattle, USA); rabbit anti-CRALBP (UW55; 1:10 000, gift from J.C. Saari, University of Washington, Seattle, USA); mouse anti-Rho (4D2) (1:8000, gift from D. Hicks, Université Louis Pasteur, Strasbourg, France) and β-actin as standard (1: 1000, Santa Cruz, USA). At least three animals were analyzed per genotype.

Rhodopsin steady-state levels and rhodopsin regeneration kinetics

Mice were dark adapted for 24 h, sacrificed under dim red light, and retinas were isolated through a slit in the cornea. Rhodopsin content was analyzed as described earlier (27). The kinetics of rhodopsin regeneration after bleaching was analyzed as previously described in detail (27). Briefly, mice were dark adapted for 24 h and pupils were dilated 30–60 min prior to light exposure. Animals were exposed for 10 min to 5000 lux of fluorescent white light. Following illumination, mice were placed in darkness for the times indicated in the results and rhodopsin content was analyzed as described above. Non-exposed mice served as dark controls. At least three animals were analyzed per condition and genotype.

Histology

Animals were sacrificed and the superior part of the eye was marked for orientation. The enucleated eyes were fixed overnight in 2.5% glutaraldehyde prepared in 0.1 M cacodylate buffer and processed as described previously (50). Semi-thin sections (0.5 μm) of Epon-embedded tissue were prepared from the inferior central retina, counterstained with Methylene blue and analyzed using a microscope (Axiovision, Zeiss, Jena, Germany). For electron microscopy, thin sections were analyzed using a Hitachi 7000 electron microscope (Hitachi, Tokyo, Japan).

Immunofluorescence

Enucleated eyes were immersed in cryoprotective medium (Jung, Nussloch, Germany) and processed for immunofluorescence as described recently (29). For detection, rabbit anti-RPE65 primary antibody (1:500) and Cy3 conjugated anti-rabbit secondary antibody (Jackson ImmunoResesarch, Soham, UK) were applied. Immunofluorescence was analyzed on a microscope (Axiovision, Zeiss) and documented using a digital imaging system.

HPLC determination of retinoids

Mice were dark-adapted for 24 h. All steps were carried out under dim red light. Animals were sacrificed, and lens and vitreous were removed from the eye through a slit in the cornea. The rest of the tissue including the retina and eyecup was snap frozen in liquid nitrogen until further analysis. Retinoid extraction and HPLC analysis was performed as previously described (27).

ERG functional tests

ERGs were recorded binocularly according to previously described procedures (6) in anesthetized mice with dilated pupils using a Ganzfeld bowl, a DC amplifier and a PC-based control and recording unit (Toennies Multiliner Vision; Viasys Healthcare, Höchberg, Germany). Recordings were obtained in both scotopic (dark-adapted overnight) and photopic (light-adapted 10 min at 30 cd s/m^2) conditions.

Single white-flash stimulus intensity ranged from −4 to 1.5 log cd s/m^2 under scotopic and from −2 to 4 log cd s/m^2 under photopic conditions, divided into 10 and 13 steps, respectively. Ten responses per intensity were averaged with an inter-stimulus interval of either 5 or 17 s (>1 cd s/m^2). At least three animals per genotype and age were analyzed.

ACKNOWLEDGEMENTS

The authors thank Coni Imsand, Gaby Hoegger, Philipp Huber and Hedwig Wariwoda for excellent technical assistance. Dr Birgit Lederman (University of Zurich) is acknowledged for help with generation of R91W knock-in animals, Sarah Habegger (Nagerzentrum) for assistance in propagation of the mutant line and Dr Andreas Zurlinden (University of Zurich) for providing Neo and DT plasmid vectors. We

thank Professor Klara Landau (Department of Opthalmology) for constant support.

Conflict of Interest statement. None declared.

FUNDING

This study was supported by the Swiss National Science Foundation (3100A0-105793) and the German Research Foundation (DFG) (RE318/2; Se837/4-1, 5-1, and 6-1, Li956-2).

REFERENCES

1. Lamb, T.D. and Pugh, E.N., Jr. (2004) Dark adaptation and the retinoid cycle of vision. *Prog. Retin. Eye Res.*, **23**, 307–380.
2. Jin, M., Li, S., Moghrabi, W.N., Sun, H. and Travis, G.H. (2005) Rpe65 is the retinoid isomerase in bovine retinal pigment epithelium. *Cell*, **122**, 449–459.
3. Moiseyev, G., Chen, Y., Takahashi, Y., Wu, B.X. and Ma, J.X. (2005) RPE65 is the isomerohydrolase in the retinoid visual cycle. *Proc. Natl Acad. Sci. USA*, **102**, 12413–12418.
4. Redmond, T.M., Poliakov, E., Yu, S., Tsai, J.Y., Lu, Z. and Gentleman, S. (2005) Mutation of key residues of RPE65 abolishes its enzymatic role as isomerohydrolase in the visual cycle. *Proc. Natl Acad. Sci. USA*, **102**, 13658–13663.
5. Redmond, T.M., Yu, S., Lee, E., Bok, D., Hamasaki, D., Chen, N., Goletz, P., Ma, J.X., Crouch, R.K. and Pfeifer, K. (1998) Rpe65 is necessary for production of 11-*cis*-vitamin A in the retinal visual cycle. *Nat. Genet.*, **20**, 344–351.
6. Seeliger, M.W., Grimm, C., Stahlberg, F., Friedburg, C., Jaissle, G., Zrenner, E., Guo, H., Reme, C.E., Humphries, P., Hofmann, F., Biel, M., Fariss, R.N., Redmond, T.M. and Wenzel, A. (2001) New views on RPE65 deficiency: the rod system is the source of vision in a mouse model of Leber congenital amaurosis. *Nat. Genet.*, **29**, 70–74.
7. Zernant, J., Kulm, M., Dharmaraj, S., den Hollander, A.I., Perrault, I., Preising, M.N., Lorenz, B., Kaplan, J., Cremers, F.P., Maumenee, I., Koenekoop, R.K. and Allikmets, R. (2005) Genotyping microarray (disease chip) for leber congenital amaurosis: detection of modifier alleles. *Invest. Ophthalmol. Vis. Sci.*, **46**, 3052–3059.
8. Thompson, D.A., Gyurus, P., Fleischer, L.L., Bingham, E.L., McHenry, C.L., Apfelstedt-Sylla, E., Zrenner, E., Lorenz, B., Richards, J.E., Jacobson, S.G., Sieving, P.A. and Gal, A. (2000) Genetics and phenotypes of RPE65 mutations in inherited retinal degeneration. *Invest. Ophthalmol. Vis. Sci.*, **41**, 4293–4299.
9. Morimura, H., Fishman, G.A., Grover, S.A., Fulton, A.B., Berson, E.L. and Dryja, T.P. (1998) Mutations in the RPE65 gene in patients with autosomal recessive retinitis pigmentosa or leber congenital amaurosis. *Proc. Natl Acad. Sci. USA*, **95**, 3088–3093.
10. Lorenz, B., Gyurus, P., Preising, M., Bremser, D., Gu, S., Andrassi, M., Gerth, C. and Gal, A. (2000) Early-onset severe rod-cone dystrophy in young children with RPE65 mutations. *Invest. Ophthalmol. Vis. Sci.*, **41**, 2735–2742.
11. Thompson, D.A. and Gal, A. (2003) Vitamin A metabolism in the retinal pigment epithelium: genes, mutations, and diseases. *Prog. Retin. Eye Res.*, **22**, 683–703.
12. Pang, J.J., Chang, B., Hawes, N.L., Hurd, R.E., Davisson, M.T., Li, J., Noorwez, S.M., Malhotra, R., McDowell, J.H., Kaushal, S., Hauswirth, W.W., Nusinowitz, S., Thompson, D.A. and Heckenlively, J.R. (2005) Retinal degeneration 12 (rd12): a new, spontaneously arising mouse model for human Leber congenital amaurosis (LCA). *Mol. Vis.*, **11**, 152–162.
13. Aguirre, G.D., Baldwin, V., Pearce-Kelling, S., Narfstrom, K., Ray, K. and Acland, G.M. (1998) Congenital stationary night blindness in the dog: common mutation in the *RPE65* gene indicates founder effect. *Mol. Vis.*, **4**, 23.
14. Pang, J.J., Chang, B., Kumar, A., Nusinowitz, S., Noorwez, S.M., Li, J., Rani, A., Foster, T.C., Chiodo, V.A., Doyle, T., Li, H., Malhotra, R., Tusner, J., McDowell, J.H., Min, S.H., Li, Q., Kaushal, S. and Hauswirth, W.W. (2005) Gene therapy restores vision-dependent behavior as well as retinal structure and function in a mouse model of RPE65 Leber congenital amaurosis. *Mol. Ther.*, **13**, 565–572.
15. Dejneka, N.S., Surace, E.M., Aleman, T.S., Cideciyan, A.V., Lyubarsky, A., Savchenko, A., Redmond, T.M., Tang, W., Wei, Z., Rex, T.S., Glover, E., Maguire, A.M., Pugh, E.N., Jr., Jacobson, S.G. and Bennett, J. (2004) *In utero* gene therapy rescues vision in a murine model of congenital blindness. *Mol. Ther.*, **9**, 182–188.
16. Lai, C.M., Yu, M.J., Brankov, M., Barnett, N.L., Zhou, X., Redmond, T.M., Narfstrom, K. and Rakoczy, P.E. (2004) Recombinant adeno-associated virus type 2-mediated gene delivery into the Rpe65$^{-/-}$ knockout mouse eye results in limited rescue. *Genet. Vaccines Ther.*, **2**, 3.
17. Chen, Y., Moiseyev, G., Takahashi, Y. and Ma, J.X. (2006) RPE65 gene delivery restores isomerohydrolase activity and prevents early cone loss in Rpe65−/− mice. *Invest. Ophthalmol. Vis. Sci.*, **47**, 1177–1184.
18. Bemelmans, A.P., Kostic, C., Crippa, S.V., Hauswirth, W.W., Lem, J., Munier, F.L., Seeliger, M.W., Wenzel, A. and Arsenijevic, Y. (2006) Lentiviral gene transfer of RPE65 rescues survival and function of cones in a mouse model of Leber congenital amaurosis. *PLoS Med.*, **3**, e347.
19. Acland, G.M., Aguirre, G.D., Ray, J., Zhang, Q., Aleman, T.S., Cideciyan, A.V., Pearce-Kelling, S.E., Anand, V., Zeng, Y., Maguire, A.M., Jacobson, S.G., Hauswirth, W.W. and Bennett, J. (2001) Gene therapy restores vision in a canine model of childhood blindness. *Nat. Genet.*, **28**, 92–95.
20. Narfstrom, K., Katz, M.L., Bragadottir, R., Seeliger, M., Boulanger, A., Redmond, T.M., Caro, L., Lai, C.M. and Rakoczy, P.E. (2003) Functional and structural recovery of the retina after gene therapy in the RPE65 null mutation dog. *Invest. Ophthalmol. Vis. Sci.*, **44**, 1663–1672.
21. Acland, G.M., Aguirre, G.D., Bennett, J., Aleman, T.S., Cideciyan, A.V., Bennicelli, J., Dejneka, N.S., Pearce-Kelling, S.E., Maguire, A.M., Palczewski, K., Hauswirth, W.W. and Jacobson, S.G. (2005) Long-term restoration of rod and cone vision by single dose rAAV-mediated gene transfer to the retina in a canine model of childhood blindness. *Mol. Ther.*, **12**, 1072–1082.
22. Narfstrom, K., Vaegan, Katz, V.M., Bragadottir, R., Rakoczy, E.P. and Seeliger, M. (2005) Assessment of structure and function over a 3-year period after gene transfer in RPE65−/− dogs. *Doc. Ophthalmol.*, **111**, 39–48.
23. El Matri, L., Ambresin, A., Schorderet, D.F., Kawasaki, A., Seeliger, M.W., Wenzel, A., Arsenijevic, Y., Borruat, F.X. and Munier, F.L. (2006) Phenotype of three consanguineous Tunisian families with early-onset retinal degeneration caused by an R91W homozygous mutation in the RPE65 gene. *Graefes Arch. Clin. Exp. Ophthalmol.*, **244**, 1104–1112.
24. Scheel, J.R., Garrett, L.J., Allen, D.M., Carter, T.A., Randolph-Moore, L., Gambello, M.J., Gage, F.H., Wynshaw-Boris, A. and Barlow, C. (2003) An inbred 129SvEv GFPCre transgenic mouse that deletes *lox*P-flanked genes in all tissues. *Nucleic Acids Res.*, **31**, e57.
25. Saari, J.C. (2000) Biochemistry of visual pigment regeneration: the Friedenwald lecture. *Invest. Ophthalmol. Vis. Sci.*, **41**, 337–348.
26. Van Hooser, J.P., Liang, Y., Maeda, T., Kuksa, V., Jang, G.F., He, Y.G., Rieke, F., Fong, H.K., Detwiler, P.B. and Palczewski, K. (2002) Recovery of visual functions in a mouse model of Leber congenital amaurosis. *J. Biol. Chem.*, **277**, 19173–19182.
27. Wenzel, A., Oberhauser, V., Pugh, E.N., Jr., Lamb, T.D., Grimm, C., Samardzija, M., Fahl, E., Seeliger, M.W., Reme, C.E. and von Lintig, J. (2005) The retinal G protein-coupled receptor (RGR) enhances isomerohydrolase activity independent of light. *J. Biol. Chem.*, **280**, 29874–29884.
28. Chen, P., Hao, W., Rife, L., Wang, X.P., Shen, D., Chen, J., Ogden, T., Van Boemel, G.B., Wu, L., Yang, M. and Fong, H.K. (2001) A photic visual cycle of rhodopsin regeneration is dependent on Rgr. *Nat. Genet.*, **28**, 256–260.
29. Wenzel, A., von Lintig, J., Oberhauser, V., Tanimoto, N., Grimm, C. and Seeliger, M.W. (2007) RPE65 is essential for the function of cone photoreceptors in NRL-deficient mice. *Invest. Ophthalmol. Vis. Sci.*, **48**, 534–542.
30. Wenzel, A., Grimm, C., Samardzija, M. and Reme, C.E. (2003) The genetic modifier Rpe65Leu(450): effect on light damage susceptibility in c-Fos-deficient mice. *Invest. Ophthalmol. Vis. Sci.*, **44**, 2798–2802.
31. Lyubarsky, A.L., Savchenko, A.B., Morocco, S.B., Daniele, L.L., Redmond, T.M. and Pugh, E.N., Jr. (2005) Mole quantity of RPE65 and its productivity in the generation of 11-*cis*-retinal from retinyl esters in the living mouse eye. *Biochemistry*, **44**, 9880–9888.

32. Machida, S., Kondo, M., Jamison, J.A., Khan, N.W., Kononen, L.T., Sugawara, T., Bush, R.A. and Sieving, P.A. (2000) P23H rhodopsin transgenic rat: correlation of retinal function with histopathology. *Invest. Ophthalmol. Vis. Sci.*, **41**, 3200–3209.
33. Hamel, C., Marlhens, F., Griffoin, J., Bareil, C., Claustres, M. and Arnaud, B. (1999) Different mutations in RPE65 are associated with variability in the severity of retinal dystrophy. In Hollyfield, J., Anderson, R. and LaVail, M. (eds), *Retinal Degenerative Diseases and Experimental Therapy*. Kluwer Academic/Plenum, New York, pp. 27–33.
34. Wenzel, A., Reme, C.E., Williams, T.P., Hafezi, F. and Grimm, C. (2001) The Rpe65 Leu450Met variation increases retinal resistance against light-induced degeneration by slowing rhodopsin regeneration. *J. Neurosci.*, **21**, 53–58.
35. Paunescu, K., Wabbels, B., Preising, M.N. and Lorenz, B. (2005) Longitudinal and cross-sectional study of patients with early-onset severe retinal dystrophy associated with RPE65 mutations. *Graefes Arch. Clin. Exp. Ophthalmol.*, **243**, 417–426.
36. Fan, J., Rohrer, B., Moiseyev, G., Ma, J.X. and Crouch, R.K. (2003) Isorhodopsin rather than rhodopsin mediates rod function in RPE65 knock-out mice. *Proc. Natl Acad. Sci. USA*, **100**, 13662–13667.
37. Takahashi, Y., Moiseyev, G., Chen, Y. and Ma, J.X. (2005) Identification of conserved histidines and glutamic acid as key residues for isomerohydrolase activity of RPE65, an enzyme of the visual cycle in the retinal pigment epithelium. *FEBS Lett.*, **579**, 5414–5418.
38. Chen, Y., Moiseyev, G., Takahashi, Y. and Ma, J.X. (2006) Impacts of two point mutations of RPE65 from Leber's congenital amaurosis on the stability, subcellular localization and isomerohydrolase activity of RPE65. *FEBS Lett.*, **580**, 4200–4204.
39. Takahashi, Y., Chen, Y., Moiseyev, G. and Ma, J.X. (2006) Two point mutations of RPE65 from patients with retinal dystrophies decrease the stability of RPE65 protein and abolish its isomerohydrolase activity. *J. Biol. Chem.*, **281**, 21820–21826.
40. Bond, R.A., Leff, P., Johnson, T.D., Milano, C.A., Rockman, H.A., McMinn, T.R., Apparsundaram, S., Hyek, M.F., Kenakin, T.P., Allen, L.F. and Lefkowitz, R.J. (1995) Physiological effects of inverse agonists in transgenic mice with myocardial overexpression of the beta 2-adrenoceptor. *Nature*, **374**, 272–276.
41. Kefalov, V.J., Carter Cornwall, M. and Crouch, R.K. (1999) Occupancy of the chromophore binding site of opsin activates visual transduction in rod photoreceptors. *J. Gen. Physiol.*, **113**, 491–503.
42. Mata, N.L., Radu, R.A., Clemmons, R.C. and Travis, G.H. (2002) Isomerization and oxidation of vitamin a in cone-dominant retinas: a novel pathway for visual-pigment regeneration in daylight. *Neuron*, **36**, 69–80.
43. Kefalov, V.J., Estevez, M.E., Kono, M., Goletz, P.W., Crouch, R.K., Cornwall, M.C. and Yau, K.W. (2005) Breaking the covalent bond–a pigment property that contributes to desensitization in cones. *Neuron*, **46**, 879–890.
44. Ma, J., Xu, L., Othersen, D.K., Redmond, T.M. and Crouch, R.K. (1998) Cloning and localization of RPE65 mRNA in salamander cone photoreceptor cells1. *Biochim. Biophys. Acta*, **1443**, 255–261.
45. Znoiko, S.L., Crouch, R.K., Moiseyev, G. and Ma, J.X. (2002) Identification of the RPE65 protein in mammalian cone photoreceptors. *Invest. Ophthalmol. Vis. Sci.*, **43**, 1604–1609.
46. Hemati, N., Feathers, K.L., Chrispell, J.D., Reed, D.M., Carlson, T.J. and Thompson, D.A. (2005) RPE65 surface epitopes, protein interactions, and expression in rod- and cone-dominant species. *Mol. Vis.*, **11**, 1151–1165.
47. Woodruff, M.L., Wang, Z., Chung, H.Y., Redmond, T.M., Fain, G.L. and Lem, J. (2003) Spontaneous activity of opsin apoprotein is a cause of Leber congenital amaurosis. *Nat. Genet.*, **35**, 158–164.
48. Boulanger, A., Liu, S., Yu, S. and Redmond, T.M. (2001) Sequence and structure of the mouse gene for RPE65. *Mol. Vis.*, **7**, 283–287.
49. Deng, C., Wynshaw-Boris, A., Zhou, F., Kuo, A. and Leder, P. (1996) Fibroblast growth factor receptor 3 is a negative regulator of bone growth. *Cell*, **84**, 911–921.
50. Samardzija, M., Wenzel, A., Aufenberg, S., Thiersch, M., Reme, C. and Grimm, C. (2006) Differential role of Jak-STAT signaling in retinal degenerations. *FASEB J.*, **20**, 2411–2413.
51. Samardzija, M., Wenzel, A., Thiersch, M., Frigg, R., Reme, C. and Grimm, C. (2006) Caspase-1 ablation protects photoreceptors in a model of autosomal dominant retinitis pigmentosa. *Invest. Ophthalmol. Vis. Sci.*, **47**, 5181–5190.